Hindawi
Mathematical Problems in Engineering
Volume 2022, Article ID 7856299, 9 pages
https://doi.org/10.1155/2022/7856299

Research Article

Research on the Influencing Factors of Motion Characteristics and Buffering of Electromagnetic Repulsion Mechanism of High Voltage Circuit Breakers

Hongkui Yan,[1,2] **Xin Lin**,[1] **and Jianyuan Xu**[1]

[1]*Liaoning Province Key Laboratory of Power Grid Safe Operation and Monitoring, Shenyang University of Technology, Shenyang 110870, China*
[2]*School of Automation, Shenyang Institute of Engineering, Shenyang 110136, China*

Correspondence should be addressed to Hongkui Yan; yanhk@126.com

Received 27 March 2022; Accepted 24 May 2022; Published 8 June 2022

Academic Editor: Jesus Valdez-Resendiz

Based on the working principle of high-speed electromagnetic repulsion mechanism, the main factors influencing the motion characteristics of the repulsion mechanism and their variation rules are analyzed and verified through calculation and simulation. Because of its fast moving speed and large kinetic energy of moving parts, it will produce large operating impact and bounce. Buffer performance is of great significance to the safe and reliable operation of high-voltage circuit breakers. Moreover, aiming at the above problems, this article studies the repulsive mechanism and its buffer problem. First, the mathematical model of the electromagnetic repulsive opening mechanism is established, and the electromagnetic repulsive force of the electromagnetic repulsive opening mechanism is deduced. The simplified model of the electromagnetic repulsive mechanism and the finite element simulation mesh are divided, and the discharge circuit model of the energy storage capacitor is designed. Then, the simulation results show that as the repulsion disk spacing, radius, storage, capacitor voltage, turn ratio, and other parameters adjust, the peak value of electromagnetic repulsion force increases, which can reach more than 60 kN, and the displacement of the mechanism can reach 84 mm within 5.5 ms. Finally, the drop weight contrast test is carried out. When the landing height is 300 mm, 500 mm, and 700 mm, respectively, the energy absorption rate of the buffer in the three groups of tests is higher than 85%. Through the speed curve simulation after the installation of buffer, it is verified that the elastic clay buffer is suitable for the buffer mode of fast switch, and a high-speed buffer device based on the elastic clay material is proposed.

1. Introduction

At present, for the high-voltage vacuum circuit breaker, the operating mechanism can minimize or even eliminate the unstable fluctuation of the power system during the opening process. The research on the operation mechanism of the circuit breaker has attracted the attention of the relevant technicians. With the increasing fault current, a matching fast switch is needed. At present, the high-speed repulsion mechanism with microsecond response speed is a common practice. Its fast starting speed and pulse output characteristics match well with the opening reaction characteristics of the vacuum switch, which meets the requirements of fast opening [1–5]. Due to the large kinetic energy of its moving parts, it will produce large operating impact and bounce. Taking an effective cushioning method can reduce the rebound of the moving parts of the electromagnetic repulsion mechanism and increase the service life of the bellows of the vacuum interrupter. Especially with the continuous development of the moving speed of the electromagnetic repulsion mechanism at high speed, the appropriate cushioning method is particularly important [6].

The common buffering methods of electromagnetic repulsion mechanism are spring buffering, polyurethane buffering, electromagnetic buffering, and so on. Spring buffering method is easy to cause component rebound; with the increase of buffer times, the recovery of deformation rate is worse; although the electromagnetic buffer has good

buffering effect, the wiring line to meet its buffering is complex. The studies in references [7, 8] show that elastic cement is a new type of organic material with elasticity, fluidity, and compressibility. The elastic mastic has large elasticity, which can effectively buffer the action of external forces through shrinkage. The elastic mastic has high viscosity, is easy to form, has large viscosity adjustment, has friction force, and is convenient to buffer large impact energy. This article attempts to study the closing bounce suppression of elastic mastic material, analyze the feasibility of using elastic mastic buffer as a buffer device, and make it possible to use it as a buffer device of electromagnetic repulsion operating mechanism of high-voltage switch.

In this article, the electromagnetic repulsion opening mechanism model is established through Maxwell simulation software, the structure of the electromagnetic repulsion mechanism is designed, and the electrical parameters are calculated, and the corresponding simulation analysis diagram and the dynamic characteristic simulation diagram of the opening process of the repulsion mechanism are obtained. It is found that the initial distance between the repulsion disk and the coil is inversely proportional to the electromagnetic repulsion force. A large electromagnetic repulsion force can be obtained when the radius of the repulsion disk is similar to that of the coil. The thickness of the repulsion disk should be selected according to the skin effect of the eddy current. There are extreme values for the number of turns and coil thickness of the driving coil. Increasing the voltage and capacity of the energy storage capacitor can improve the electromagnetic repulsion [9, 10]. Combined with the characteristics of the electromagnetic repulsion mechanism, special requirements are put forward for the buffer, which should have both small restoring force and large compression process output. On this basis, an elastic mastic buffer is designed to meet the high-speed buffer requirements of the electromagnetic repulsion mechanism. At the same time, the buffer capacity of the high-speed buffer device is verified by experimental means.

2. Structure and Principle of Repulsive Mechanism

2.1. Working Principle. The structure of the repulsion mechanism is shown in Figure 1. It is mainly composed of three parts: the first part is the vacuum arc extinguishing chamber, which mainly includes dynamic and static contacts and their respective contact springs. The dynamic and static contacts complete the on-off of the circuit, and the contact spring plays the role of buffering, maintaining contact, and restraining bounce. The second part is the electromagnetic repulsion mechanism, which drives the dynamic and static contacts to complete the opening function through the movement of the repulsion plate. The working principle is as follows: control the G1 conduction of IGBT device, charge the capacitor C by power V, disconnect G1 after charging, and control the thyristor VT1 on, and capacitor C discharges the breaking coil plate. The eddy current generated in the repulsion disk interacts with the magnetic field to form an electromagnetic repulsion force, which makes the repulsion disk move down quickly and quickly and drives the contact to quickly break off [11–14]. The free-wheeling diode VD1 prevents the capacitor from charging in the reverse direction and then turns off the thyristor VT1 to complete the breaking process. The third part is the buffer mechanism device. The single output rod damping ring elastic mastic buffer is adopted. When the elastic mastic buffer is stressed, the elastic mastic is squeezed. When the external force is removed, the compressed elastic mastic expands, and the buffer returns to its original position.

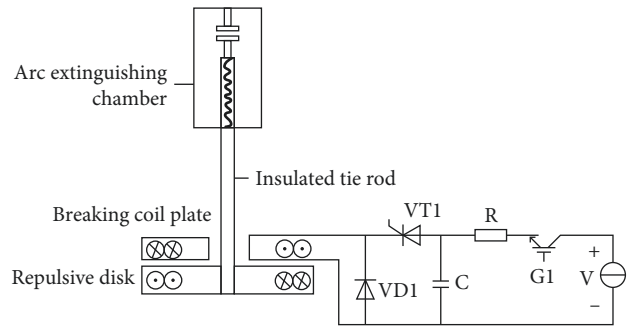

Figure 1: Structure diagram of the repulsion mechanism.

The schematic diagram of the electromagnetic repulsion mechanism is shown in Figure 2, and its relevant parameters are shown in Table 1.

2.2. Mathematical Model of Electromagnetic Repulsion. Figure 3 shows the equivalent excitation circuit of the electromagnetic repulsive opening mechanism. Similar to the excitation source, the capacitor is also connected with the opening repulsion coil to form a pulse discharge circuit. When the opening action is required, the capacitor discharges and generates a pulse current $i_1(t)$ in the opening coil L_1, which are represented by the resistance R_1 and self-inductance L_1 of the opening coil, respectively. The electromagnetic repulsion disk is equivalent to the induction circuit. When the pulse current flows through the opening coil L_1, the induced current $i_2(t)$ is generated in the repulsion disk. In Figure 3, the equivalent resistance R_2 and self-induction L_2 are highlighted [15–17]. Mutual inductance is observed between the opening coil and the electromagnetic repulsion disk. M in Figure 3 denotes the mutual inductance between the opening coil and the electromagnetic repulsion disk, and its coupling degree is closely related to the distance between them. The electromagnetic repulsion disk moves away from the coil when the mechanism opens. With the increase of movement time, the distance between the two keeps increasing, and the mutual inductance m becomes smaller [18, 19].

The following equivalent equation of the electromagnetic repulsion mechanism can be obtained according to Kirchhoff's circuit theorem:

$$\begin{aligned} i_1(t)R_1 + L_1\frac{di_1(t)}{dt} + M\frac{di_2(t)}{dt} &= u(t), \\ i_2(t)R_2 + L_2\frac{di_2(t)}{dt} + M\frac{di_1(t)}{dt} &= 0. \end{aligned} \tag{1}$$

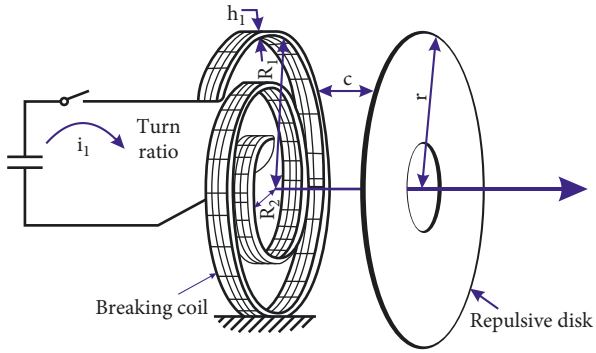

Figure 2: Schematic diagram of electromagnetic repulsion mechanism.

Table 1: Main parameters of the model.

Parameter	Numerical value
Turn ratio	18
Coil thickness h (mm)	27
Repulsion disc thickness h_1 (mm)	15
Repulsion disk radius r (mm)	110
Outer radius of coil R_1 (mm)	85
Inner radius of coil R_2 (mm)	55
Clearance between coil and repulsion disc c (mm)	1.2
Mass of movable part (repulsion disc, pull rod) (m/g)	1770

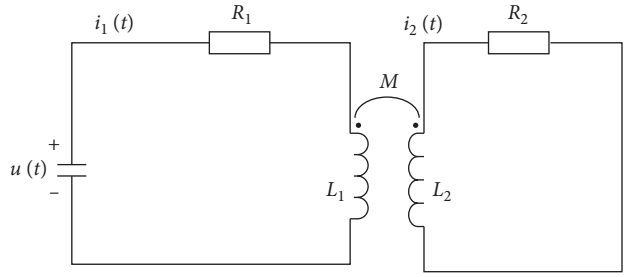

Figure 3: Equivalent circuit of electromagnetic repulsion mechanism.

including voltage at both ends of capacitor $U(t) = u_0 - 1/C \int_0^t i_1(\tau)d\tau$, u_0 is the initial charging voltage at both ends of the capacitor. When the electromagnetic repulsive opening mechanism opens, the power supply releases energy and provides the movement energy for the mechanism and other forms of energy consumption. Assuming that the energy released by the power supply is dJ, the work done by the mechanism is dA, the energy change in the magnetic field is dW, and the heat loss is dQ, and the law of conservation of energy can be expressed as

$$dJ = dA + dW + dQ. \tag{2}$$

The energy released by the power supply is expressed as

$$\begin{aligned} dJ = {} & i_1(t)R_1dt + i_2(t)R_2dt + i_1(t)L_1di_1(t) \\ & + i_1(t)Mdi_2(t) + i_2(t)L_2di_2(t) \\ & + i_2(t)Mdi_1(t) + 2i_1(t)i_2(t)dM. \end{aligned} \tag{3}$$

The magnetic energy between the coil and the repulsive disk can be expressed as

$$\begin{aligned} L_1dW = {} & i_1(t)L_1di_1(t) + i_2(t)L_2di_2(t) + i_1(t)Mdi_2(t) \\ & + i_2(t)Mdi_1(t) + i_1(t)i_2(t)dM. \end{aligned} \tag{4}$$

The expression of heat loss is as follows:

$$dQ = i_1^2(t)R_1dt + i_2^2(t)R_2dt. \tag{5}$$

The work expression of the mechanism can be determined by simultaneous equations (3)–(5) as follows:

$$dA = i_1(t)i_2(t)dM. \tag{6}$$

Hence, the electromagnetic repulsive force of the electromagnetic repulsive opening mechanism is as follows:

$$F = \frac{dA}{dx} = i_1(t)i_2(t)\frac{dM}{dx}. \tag{7}$$

According to the electromagnetic repulsion formula (7), the electromagnetic repulsion F is directly proportional to the current flowing through the opening coil $i_1(t)$, the induced current generated in the repulsion disk $i_2(t)$, the mutual inductance between the opening coil and the electromagnetic repulsion disk, and the derivative $\mathrm{d}M\mathrm{d}x$ of the distance between the repulsion disk and the coil.

2.3. Analysis and Design of the Simulation Model of Repulsion Mechanism

2.3.1. Simulation Model. In this paper, a two-dimensional axisymmetric geometric model is established by using Maxwell electromagnetic field simulation software. After preliminary calculation of the model parameters and comprehensive consideration of the feasibility of project implementation, the preliminary parameters and size range are obtained. The repulsion disk is a metal disk of aluminum alloy. The simplified model of electromagnetic repulsion mechanism and finite element simulation grid division are shown in Figure 4.

The circuit is set, as the precharged energy storage capacitor is connected in series with the excitation coil, the rated voltage of the capacitor is 500 V, and the capacitance capacity is 38 mF. At the same time, when simulating the dynamic characteristics of the opening process, Table 2 shows the relationship between the number of turns of the opening coil and the maximum electromagnetic force, the average speed of the iron core, and the moving distance of the iron core under the determination of the initial voltage and capacity of the capacitor.

It can be seen from Table 2 that when the opening coil turns 8 and 13, the moving distance of the moving iron core cannot reach the contact breaking distance required by the vacuum interrupter; when the wire turns 23 and 28, although the contact breaking distance required by the vacuum

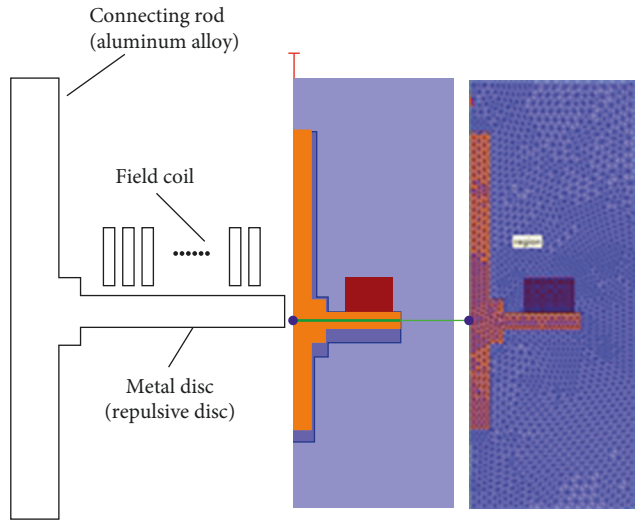

Figure 4: Geometric model and mesh of the electromagnetic repulsion mechanism.

Table 2: Relationship between turn number of switching coil and electromagnetic.

Turn ratio	Maximum electromagnetic force (kN)	Average velocity (m/s)	Moving distance (mm)
8	20.252	—	32
13	33.335	—	61
18	44.996	15	80
23	50.234	16	80
28	56.758	17	80

interrupter is met, it causes unnecessary waste; it is more appropriate when 18 turns are taken as the wire turns of the opening coil. On the one hand, it meets the contact breaking distance required by the vacuum interrupter. At the same time, under the premise of meeting the requirements, the number of wire turns should be as few as possible to avoid material waste, reduce costs, reduce unnecessary impact force, and improve the service life of the contacts.

The simulation results of the dynamic characteristics of the opening process of the repulsive mechanism proposed in this article are shown in Figure 5, including three relationship diagrams of electromagnetic force and time, mechanism motion speed and time, and mechanism displacement and time.

It can be seen from Figure 5 that the electromagnetic repulsion force reaches the maximum value of 44.996 kN in the first 1 ms. With the movement of the repulsion plate, the electromagnetic repulsion force begins to decrease. With the reduction of the distance between the moving core and the permanent magnet, the electromagnetic force increases clearly until the end of the stroke; the maximum motion speed of the mechanism can reach 25 m/s, and the average motion speed of the whole motion stroke is 13 m/s; for the 126 kV vacuum interrupter, the contact opening distance is required to reach 60 ± 2 mm, and the overtravel is 24 ± 2 mm. According to the displacement versus time curve in Figure 5, it can reach 84 mm in a very short time, and the opening time of the mechanism is 5.5 ms, which is conducive to the rapid and accurate control of the vacuum circuit breaker.

2.4. Analysis on the Influence of Different Parameters on the Operation Process of Repulsion Mechanism. The influence of basic parameters such as coil and repulsion disc on the electromagnetic repulsion is analyzed when the electromagnetic repulsion mechanism works. In addition to the influence of the changing topology of the repulsion disk on the electromagnetic repulsion force, its initial position, that is, the distance from the driving coil, also has a great influence on the electromagnetic repulsion force; the topological structure of the driving coil has an obvious influence on the electromagnetic repulsion force, and its main parameters have a great influence on the peak value of the electromagnetic repulsion force, the occurrence time of the peak value of the electromagnetic repulsion force, and the duration of the electromagnetic repulsion force.

2.4.1. The Influence of Coil Turns. The influence of coil turns on the electromagnetic repulsion force is shown in Figure 6. The coil turns are initially set at 18. When the coil turns are increased to 28, the peak value of the electromagnetic repulsion force increases by nearly 3000 N, but the time lag of the peak value of the electromagnetic repulsion force is about 0.1 ms. After increasing the number of coil turns to 38, the peak value of electromagnetic repulsion force no longer increases but decreases by nearly 3000 N, and the time lag of the peak value of electromagnetic repulsion force is about 0.17 ms. When the coil turns are reduced to 8 turns, the peak value of the repulsion force decreases by nearly 20 kN, but the

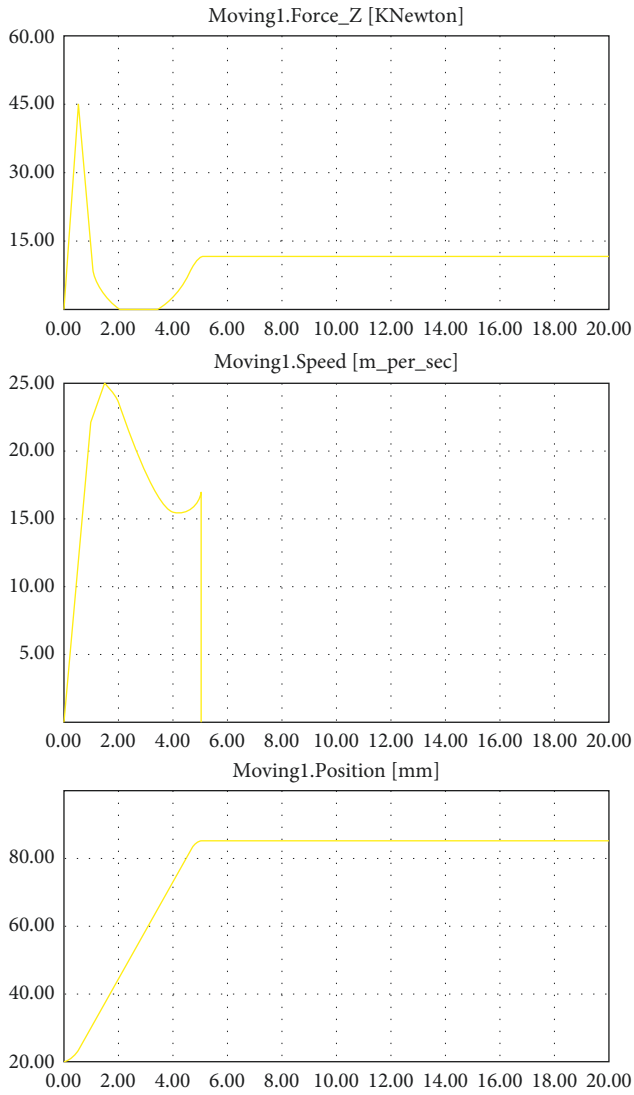

Figure 5: Dynamic characteristics of opening process.

time of the peak value of the repulsion force is about 0.1 ms ahead of time.

2.4.2. Influence of Storage Capacitor Voltage. The initial voltage of the energy storage capacitor is 500 V, with 100 V as the first gear, the lowest voltage is 300 V, and the highest voltage is 800 V. Two kinds of influences are analyzed: one is the influence of the energy storage capacitor voltage on the travel time, and the other is the influence of the energy storage capacitor voltage on the peak value of electromagnetic repulsion. Figure 7 shows the simulation results of different capacitor voltages.

As shown in Figure 7, the higher the voltage of the energy storage capacitor, the greater the peak value and the maximum velocity of the electromagnetic repulsion force. It can be seen that the electromagnetic repulsion force and velocity can be increased by increasing the voltage of the energy storage capacitor, to reduce the movement time of the moving part.

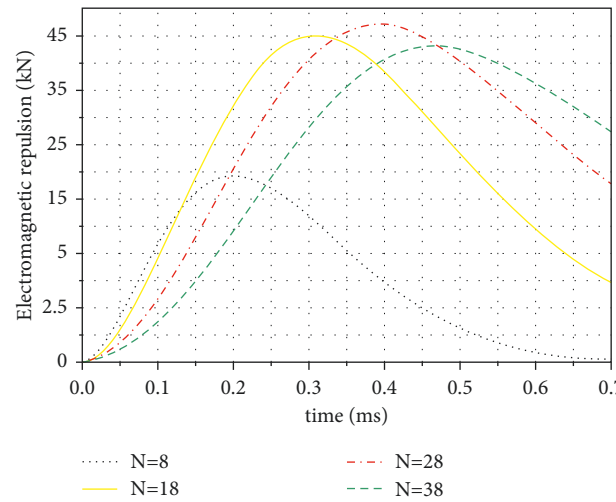

Figure 6: Influence of coil turn on electromagnetic repulsion.

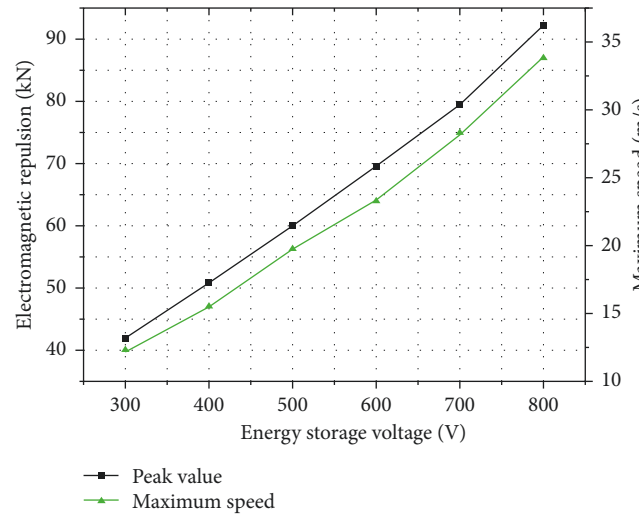

Figure 7: Influence of capacitor voltage on the peak value and maximum velocity of electromagnetic repulsion.

2.5. Influence of Repulsive Disk on Basic Parameters

2.5.1. Influence of the Distance d between the Repulsive Disk and the Coil. The electromagnetic repulsion curves of different distances between the coil and the repulsion disk are shown in Figure 8. With the increase of the distance, the peak value of the electromagnetic repulsion force decreases, and the occurrence time of the peak value of the electromagnetic repulsion force lags behind. The reason is that, with the increase of the distance, the overall inductance of the system also increases, indicating that the simulation model is in line with the actual situation.

2.5.2. Influence of Repulsive Disk Radius r. The radius of the coil in the initial model is basically the same as that of the repulsion disk, which is taken as 70 mm. The simulation diagram of the influence of the repulsion disk radius is shown in Figure 9. It can be seen from the figure that

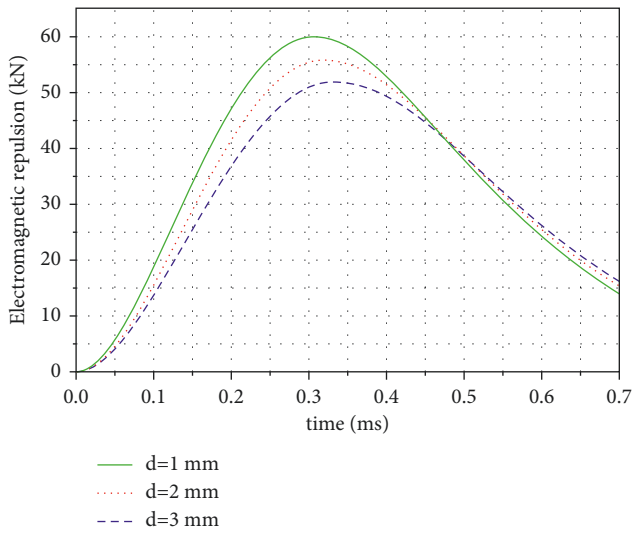

Figure 8: Influence of the distance between the repulsive disk and the coil.

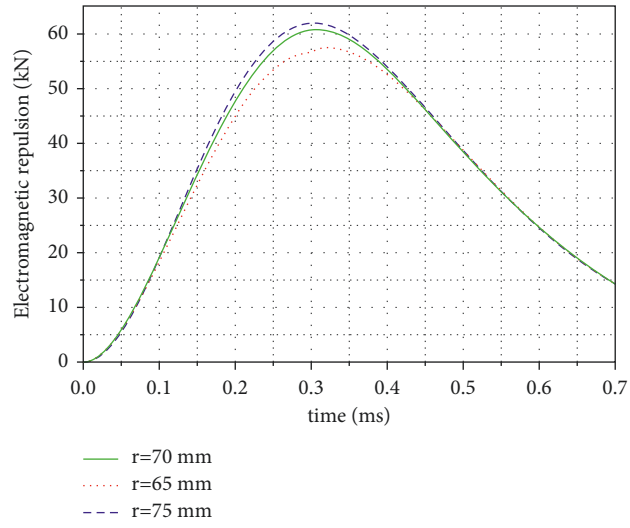

Figure 9: Influence of repulsion disk radius.

reducing the metal disk radius will lead to the reduction of the peak electromagnetic repulsion force under other conditions. However, when the radius of the metal disk becomes larger, the same effect cannot be achieved.

According to the above conclusions, the speed of the repulsion mechanism can be improved by reducing the motion mass, appropriately, increasing the thickness of the repulsion disk, increasing the number of coil turns, reducing the initial gap, and increasing the capacitor voltage. From the above simulation analysis, it is concluded that there are two methods to improve the motion speed of the repulsion mechanism: increasing the peak value of the electromagnetic repulsion or slowing down the falling speed of the electromagnetic repulsion. Increasing the inner diameter of the coil, increasing the number of turns of the coil, and increasing the thickness of the repulsion plate mainly improve the motion speed of the repulsion mechanism by slowing down the falling speed of the electromagnetic repulsion; to reduce the initial clearance, the main method is to increase the peak value of electromagnetic repulsion force to improve the motion speed of the repulsion mechanism. This method will sharply increase the peak value of electromagnetic repulsion force, which requires higher mechanical characteristics of the motion mechanism, but the speed is not improved much. The reason is that as the distance decreases, the speed reaches the limit before reaching the maximum value. Therefore, the speed does not increase significantly. Therefore, when designing the fast repulsion mechanism, the initial gap should be appropriately larger. Under the condition of ensuring that the repulsion mechanism meets the strength requirements, the thickness of the repulsion plate can be appropriately reduced.

2.6. Design and Test of Elastic Mastic Buffer. The principle of elastic mastic buffer is to inject a viscoelastic fluid damping material into the closed cavity. If it is subjected to an external force, it will push the buffer piston rod into the cavity, which will compress the damping medium in the cavity and make it change to a certain state. After the internal pressure increases, it will form a certain elastic reaction force on the piston rod; at the same time, the internal medium and damping structure will form friction, which is mainly related to the speed of motion. If the speed is higher, it will be subject to greater viscous resistance, so it will be transformed into a large amount of elastic potential energy instantaneously. In this way, the energy conversion and storage are effectively completed. [20].

A damping ring type elastic clay buffer is designed; its stroke and capacity are 200 mm and 0.15 kJ, respectively. In the actual research process, the buffering effect of the buffer is generally verified by the drop weight test. The specific process is as follows: first, the acceleration sensor is set to the impact drop weight, and then the acceleration signal of the piston rod and the drop weight in the synchronous movement process are obtained. Then, a buffer is set in the base, and the drop hammer is set at a certain height. After it falls, it will impact the piston rod. During this process, the changes of acceleration and displacement are recorded by means of acquisition devices and sensors, and the time-varying curves are obtained. When the drop hammer is still the same, the process is executed again. In this way, multiple groups of recorded data can be obtained.

In the process of the experiment, different landing heights are used for testing, which are set to 300 mm, 500 mm, and 700 mm, respectively, and then, the corresponding displacement signals are collected, and the processed displacement signals are obtained in a certain way, as shown in Figure 10. The basis for the selection of height is a single rod damping ring elastic mastic buffer with a stroke of 200 mm. The buffer performance of the buffer is measured by the limit overtravel multiples of 1.5, 2.5, and 3.5.

E is the gravitational potential energy of the falling hammer, that is, the impact energy of each time, which is directly proportional to the height and mass of the falling hammer.

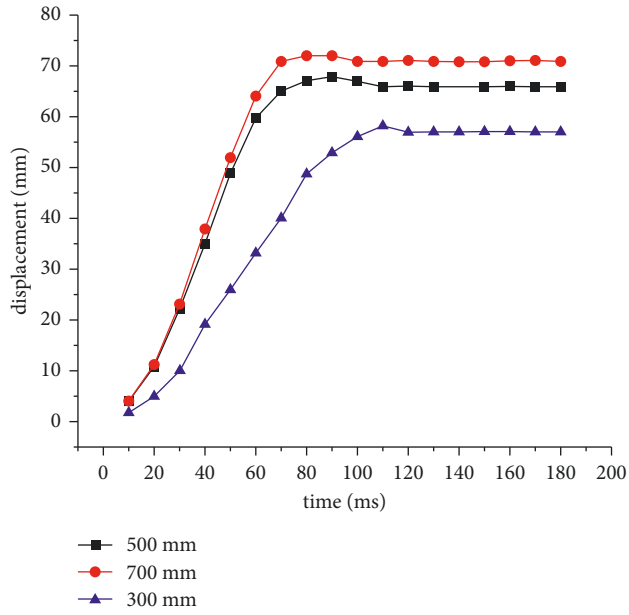

Figure 10: Displacement and time curve.

Table 3: Calculation of energy loss rate and buffer energy absorption rate.

Impact height (mm)	300	500	700
Impact energy E/J	127.6	202.6	291.5
Actual impact energy E_1/J	31.8	55.4	69.9
Energy absorbed by buffer E_0/J	28.4	48.5	60.1
Energy loss rate of friction collision η_1	75.08%	72.66%	76.02%
Energy absorption rate of buffer η	89.31%	87.55%	85.98%

$$E = mgh. \tag{8}$$

E_0 is the energy actually absorbed by the buffer; that is, it is directly proportional to the compression force and compression distance. In each impact buffering process, the area under the loading curve is the energy actually absorbed by the buffer, and the formula is as follows:

$$E_0 = \int_0^x F(x)dx. \tag{9}$$

E_1 is the actual impact energy of the falling hammer after being subjected to friction force, which is directly proportional to the mass and speed of the falling hammer. It is assumed that each impact energy E is equal to the gravitational potential energy of the falling weight. In the process of falling, part of the energy will be lost due to the effect of friction. Therefore, the energy can be calculated according to the following formula:

$$E_1 = \frac{1}{2}mv^2. \tag{10}$$

The energy loss rates corresponding to friction and buffer are, respectively, expressed as η_1, η, and the specific forms are as follows:

$$\eta_1 = \frac{E - E_1}{E}$$
$$\eta = \frac{E_0}{E_1}. \tag{11}$$

According to the above formula, the impact energy, absorbed energy, and absorption rate can be calculated, which are shown in Table 3.

According to the data in Table 3, it can be clearly seen that the energy absorbed by the buffer during the experiment is not high, only accounting for about 30% of the initial impact energy, while the other energy loss is mainly related to the friction resistance, which also accounts for a large proportion. In addition, according to the test results, the energy absorption rates of the buffers in the three groups of tests were all higher than 85%, indicating that the buffer energy achieved a good effect.

3. Experiment and Measurement of the Prototype

The elastic clay buffer is connected to the prototype of electromagnetic repulsion mechanism for opening and

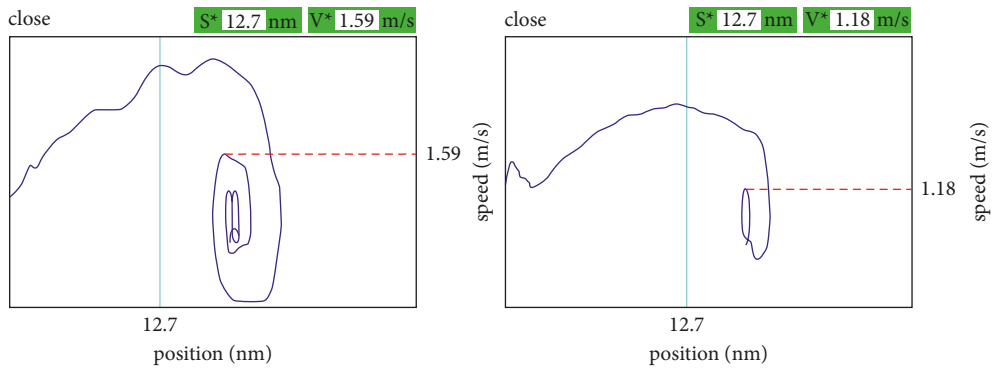

Figure 11: Moving contact closing displacement-speed curve.

closing test. Figure 11 shows the speed curve without buffer on the left and the speed curve with buffer on the right. It can be seen that, after using elastic clay buffer, the bounce of closing is clearly reduced. In the simulation environment, when the circuit breaker is at $s = 12.7$ nm, that is, when the circuit breaker is in the rigid closing position, the closing bounce amplitude decreases significantly, and the speed decreases from 1.59 m/s to 1.18 m/s.

4. Conclusion

(1) Taking a 126 kV high-voltage circuit breaker as an example, this article analyzes the composition principle of its repulsion mechanism, establishes the equivalent excitation circuit of the electromagnetic repulsion opening mechanism, divides the finite element simulation grid, designs the discharge circuit of the energy storage capacitor, and generates the dynamic characteristic simulation diagram of the opening process. It can be seen that the displacement of the mechanism reaches 84 mm in 5.5 ms.

(2) The influence of the basic parameters such as coil and repulsion disk on the electromagnetic repulsion force during the operation of the repulsion mechanism is analyzed. The research shows that increasing the energy storage capacitor voltage, reducing the distance between the repulsion disk and coil, and properly adjusting the number of coil turns can increase the peak value of electromagnetic repulsion force.

(3) A damping ring elastic mastic buffer is designed, and the corresponding prototype is developed and tested. Through the speed curve after installing the buffer, it can be seen that the bounce of closing is clearly reduced after using the elastic mastic buffer.

Data Availability

No data were used to support the findings of the study.

Conflicts of Interest

The authors declare that they have no conflicts of interest.

Acknowledgments

This work was partly supported by the National Natural Science Foundation of China (61773269), the Natural Science Foundation of Liaoning Province of China (2019-KF-03-08), the Program for Liaoning Excellent Talents in University (LR2019045), and the Program for Shenyang High Level Innovative Talents (RC190042).

References

[1] Z. Li, L. B. Y. Xianglian, and X. W. Hao, "Design and test of hybrid fast mechanism vacuum circuit breaker [J]," *High voltage technology*, vol. 44, no. 6, pp. 1797–1799, 2018.

[2] L. Hong and M. Xiren, "Research status and development trend of operating mechanism [J]," *Electrical appliances and energy efficiency management technology*, vol. 12, pp. 1–7, 2017.

[3] Y. Liu, X. J. Z. Jianying, Z. S. H. Dongpeng, and Z. Jibin, "Design of driving motor for motor operating mechanism based on Intelligent Architecture [J]," *Electrical Engineering*, vol. 2, no. 3, pp. 8–11, 2021.

[4] S. Li, Z. Y. G. Zhenxin, L. X. W. Zichi, and H. X. Z. Dapeng, "Suppression of contact overshoot and rebound in circuit breaker of motor operating mechanism [J]," *High Voltage Apparatus*, vol. 56, no. 9, pp. 273–278, 2020.

[5] T. Y Research, *On Driving Motor and Control System of Operating Mechanism of High Voltage Circuit breaker [D]*, Shenyang University of Technology, 2019.

[6] W. Wen and L. Bin, H. Y. M. Jiuxin, Research on buffer characteristics of high voltage fast switch based on bidirectional electromagnetic repulsion mechanism [J]," *Journal of Electrotechnics*, vol. 34, no. 7, pp. 1449–1458, 2019.

[7] D. Wang, T. Z. G. Yuefei, and L. Yang, "Design of shock loading buffer with elastic mortar [J]," *Hydraulic and pneumatic*, vol. 11, pp. 136–141, 2019.

[8] G. Cheng, *Study on Mechanical Model of JN30 Cement buffer [D]*, Dalian Jiaotong University, China, 2019.

[9] P. Yang and L. M. Y. Li, "Simulation analysis of the factors influencing the motion characteristics of electromagnetic repulsion mechanism[J]," *Journal of Shenyang Institute of Engineering (NATURAL SCIENCE EDITION)*, vol. 17, no. 1, pp. 51–57, 2021.

[10] B. Liu, X. Y. Haibo, and Z. C. X. Jie, "Design and experiment of high efficiency electromagnetic repulsion mechanism for engineering application[J]," *High voltage technology*, vol. 46, no. 12, pp. 4283–4290, 2020.

[11] X. Lin, *Modern High Voltage Electrical technology[M]*, China Machine Press, Beijing, China, 2011.
[12] L. S. G. Zhenxin, H. D. L. Dexiang, and H. Xiaoming, "Design of motor operating mechanism for fast grounding switch [J]," *Journal of Shenyang University of Technology*, vol. 42, no. 6, pp. 613–617, 2020.
[13] L. X. G. Zhenxin, W. Z. G. Yujing, X. J. L. Shaohua, and H. X. Q. Kai, "Research on the influence of motor torque fluctuation on the speed of circuit breaker [J]," *High Voltage Apparatus*, vol. 56, no. 7, pp. 63–68, 2020.
[14] N. Xia, J. Zou, D. Liang, Y. Gao, Z. Huang, and Y. Wang, "investigations on the safe stroke of mechanical HVDC vacuum circuit breaker," *Journal of Metals The Journal of Engineering*, no. 16, pp. 3022–3025, 2019.
[15] P. Yang, *Study on Repulsion Mechanism of Vacuum Circuit Breaker at the Outlet of High Current generator [D]*, Shenyang Institute of Engineering, 2019.
[16] Z. Zhu, C. L. Y. Zhao, and H. J. X. Ming, "Structural stress analysis and optimization design of electromagnetic repulsion mechanism [J]," *High voltage technology*, vol. 46, no. 8, pp. 2692–2699, 2020.
[17] H. Zhao, *Magnetic Field Analysis and Structure Optimization Design of Fast Repulsion mechanism [D]*, Zhengzhou University, 2020.
[18] Z. J. W. Jin and Y. Zhifang, "Optimization analysis of structural parameters of electromagnetic repulsion mechanism based on electromagnetic coupling double coil model [J]," *Power automation equipment*, vol. 39, no. 6, pp. 205–211, 2019.
[19] L. B. Wenweijie, H. Y. L. Botong, and J. Yini, "Parameter matching and optimization design of electromagnetic repulsion mechanism [J]," *Journal of Electrotechnics*, vol. 33, no. 17, pp. 4102–4112, 2018.
[20] Y. Xinlin, *Research On Driving Force Design of Electromagnetic Repulsion Mechanism Considering Reaction characteristics [D]*, Huazhong University of science and technology, 2016.